Hindawi Publishing Corporation
International Journal of Rotating Machinery
Volume 2014, Article ID 984094, 11 pages
http://dx.doi.org/10.1155/2014/984094

Research Article

Numerical Investigation: Effect of Stator Vanes on Turbocharger Turbine Performance

Ganesh Yadagiri Rapolu, Siddharth Swaminathan Balachandar, and Keerthi Vallarasu Kamaraj

Turbo Energy Limited, Old Mahabalipuram Road, Paiyanur, Kanchipuram District, Chennai, Tamil Nadu 603104, India

Correspondence should be addressed to Ganesh Yadagiri Rapolu; ganesh.yr@turboenergy.co.in

Received 9 April 2014; Revised 20 August 2014; Accepted 2 September 2014; Published 14 October 2014

Academic Editor: Tariq Iqbal

With reduced turbo lag and better transient response, the introduction of VTG stator guide vanes improved turbocharger performance at all the engine operating conditions. The VTG system accelerates and maneuvers exhaust gas flow to the turbine. Favorable flow conditions at turbine inlet created by vane shape improve turbine performance. At lower engine speed, it is observed that the pressure drop across vane system influences overall efficiency. Whereas at higher speed, the pressure drop and guide vane exit flow angle are found to determine the turbine efficiency. Successful practical operation of VTG system also depends on its ability to smoothly open and close the vanes at different gas loads. Stator vane shape greatly influences the smooth operability/controllability of vane system. In the present work, 3 symmetric vanes with different T/C ratios and 2 asymmetric vanes are analyzed. The effect of geometric changes is studied from overall turbine performance as well as VTG system performance perspective. It is observed that symmetric vanes cause higher pressure drop at lower speeds leading to lower efficiency irrespective of the vane width. It is also observed that the pressure drop characteristics and vane exit flow angle are better with the asymmetric vanes, whereas the controllability of symmetric vanes is found to be superior. Analysis methodology is presented for achieving the best compromise between performance and controllability by the modification of vane geometric parameters through CFD simulations.

1. Introduction

High boost at low engine speeds has become a necessary requirement of automotive engine manufacturers due to the demand for quick response to the vehicle operating conditions. It has been a challenge for turbocharger manufacturers to minimize or avoid turbo lag at lower engine speeds. The demand for high boost from the turbocharger within the space constraints led to the development of VTG turbocharger. It promises higher efficiency at lower engine speeds by accelerating the exhaust gas flow through the nozzle gaps formed of circular array of vanes pivoting to attain varying nozzle gap at different engine operating conditions. Varying nozzle gap helps to achieve higher compressor boost at low speeds. The performance of VTG system greatly depends on the chosen vane shape and its location. Several airfoil shaped vanes are currently being used in turbocharger application.

Typical VTG system consists of a vane ring supporting the vanes. Vane ring on one side and a flat plate on the other side enclose the vanes forming nozzle passages. It is necessary to provide appropriate clearance between the vanes and flat plate/vane ring for free motion of the vane while closing and opening. But, it is also desirable to ensure the clearance is as low as possible to reduce the tip leakage. Normally, this clearance is ensured by introducing cylindrical shaped spacers having height slightly greater than the vanes as required to achieve the clearance. Each vane is casted along with shaft which connects the vanes to the links through vane ring. Reciprocating motion from actuator (electric or vacuum/pressure based) is converted to rotational motion of link-shaft-vane assembly. For different engine operating conditions, actuator rod moves by a predetermined distance for rotating the vanes to close or open as desired. The free vortex flow from volute is led to turbine wheel through the nozzle passages formed by these stator vanes. Flow entering the

turbine wheel is greatly influenced by various geometric parameters of the vane system such as the vane shape, size, number, and PCD of vanes. Higher turbine efficiency can be achieved by optimizing these geometric parameters of the VTG system.

2. Literature

Srithar and Ricardo [1] investigated variable geometry mixed flow turbine of a turbocharger. In this research it was found that the vane surface pressure is highly affected by the flow in the volute rather than the adjacent vane surface interactions, especially at closer positions. It was also shown that substantial amount of exhaust gas energy can be recovered at velocity ratios U/C of less than 0.7. Zweifel's criterion was used for finding the number nozzle vanes or indirectly the blade spacing as an important factor in loss contribution. It was concluded that nozzle vanes experience higher pressure on suction surface than pressure surface, especially at closer positions. This is predominately due to upstream flow from the volute than the vane-to-vane flow interaction. The unsteady performance was found to show substantial deviation from the equivalent quasi-steady assumption at 40 Hz pulsating flow because of high blockage in the nozzle which consequently leads to choking and delaying of the volute emptying before the next cycle of filling.

Eleni et al. [2] evaluated the turbulence models for the simulation of flow over NACA 0012 airfoil. The behavior of 4 digit symmetric airfoil NACA 0012 at various angles of attack was studied. It was found that the most appropriate turbulence model for airfoil simulation was the k-ω SST two-equation model as it showed good agreement with the published experimental data. Initially, it was observed that the model predicted slightly higher drag coefficient as the actual airfoil has laminar flow existing over the forward half portion. So, the transition point from laminar to turbulent regime was first determined and accordingly changes were made in the computational grid splitting into two regions. Analysis with the modified computational grid showed good agreement with corresponding experimental data.

Simpson et al. [3] analyzed vaned and vaneless stators in radial inflow turbines through CFD and test. The CFD results were validated with test data. Various areas of loss generation in stators were identified and losses were quantified. 3 different vaneless volutes with symmetric cross section and linearly varying A/r ratios with azimuth angle were designed. Further, 3 different vaned stators were also designed with matching mass flow rates (at design points) to the corresponding vaneless volutes. The vaned stators contained 13 uncambered guide vanes. It was found that the vaneless stators cause lower total pressure losses. The flow through vaneless stators showed two counter rotating vortices, whereas, additional horseshoe type vortices were observed over the vanes leading to higher levels of aerodynamic losses. The static pressure distribution at the rotor inlet showed higher flow uniformity in vaneless stators and the CFD predictions were well in agreement with the test measurements. It was concluded that vaneless stators, if designed appropriately to deliver uniform flow to rotor, can deliver better performance than vaned stators.

Hu et al. [4] analyzed the effect of nozzle clearances on turbine performance numerically. For this analysis the peak efficiency point ($U/C = 0.68$) was chosen. It was found that with 2% of nozzle clearance, the peak efficiency of the rotor deteriorates by about 0.5%. With 3% of nozzle clearance, the efficiency drops by about 2% and when the nozzle clearance is increased to 4%, the efficiency drops by about 3%. The efficiency of the rotor deteriorates rapidly if the nozzle clearance is further increased. It is shown that the nozzle clearance not only leads to extra loss of efficiency due to leakage flow inside the nozzle, it also affects rotor performance. Numerically it was found that reduction in the nozzle efficiency decrement occurs gradually up to 5% clearance ratio beyond which the nozzle efficiency decrement remained constant even after any increase in the clearance ratio. It was also found that the exit flow condition of the nozzle is less uniform due to higher clearance. It increased the tangential velocity acting opposite to the wheel rotational direction causing negative incidence angle at the rotor inlet leading to higher incidence losses. It was concluded that the turbine stage performance is very sensitive to nozzle clearance; it deteriorates gradually with increase of the nozzle clearance.

3. Stator Vane Geometry

Simulations are carried out with three symmetric vanes and two asymmetric vanes. Vane shapes similar to asymmetric vanes 1 and 2 are commercially in use by turbocharger manufacturers and are used in this work for study purpose only. Figure 1 shows different vane shapes used for this study. Shapes (a), (b), and (c) are symmetric vanes with different thickness to chord length (T/C) ratios, Shapes (d) and (e) are the asymmetric vanes. Dimensions of all the vanes are approximately chosen so as to appropriately fit in the common VTG system cartridge chosen for this study.

Geometric parameters of vane system such as PCD, vane height, and clearance are maintained same for all the vanes. The solidity ratio (i.e., ratio of product of number of vanes and chord length to circumference at vane PCD) is maintained in the range of 1.07 to 1.19 by choosing the number of vanes appropriately. Vanes are distributed uniformly around the turbine wheel to ensure that the flow from all vane nozzles enters the wheel uniformly into all the wheel blade passages. Vanes are opened until a gap of 1 mm (max open) between vane trailing edge and turbine wheel leading edge and are closed until a gap of 2 mm (min open) between adjacent vanes.

Figure 2(a) shows the vane-shaft-link assembly. A collar is provided at the junction of the vane and shaft for stiffness against high gas forces. Vanes are pivoted about the shaft axis. The location of pivot point P for all the vanes was chosen so that the x/C ratio is maintained at 0.52 approximately.

4. Computational Domain & Simulation Strategy

Turbocharger turbine side flow core starting from the volute inlet up to the turbocharger outlet is extracted from the

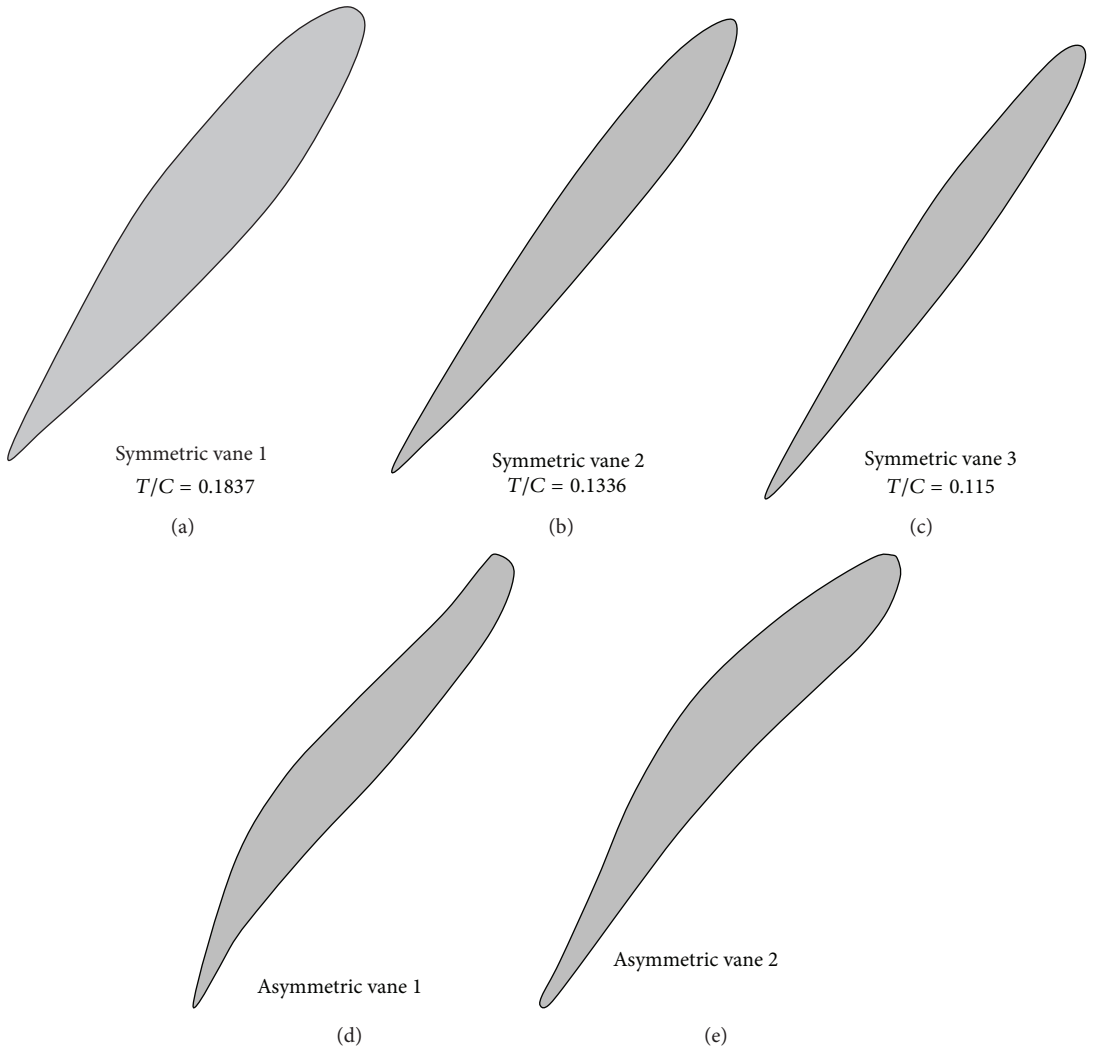

Figure 1: Different stator vane shapes studied.

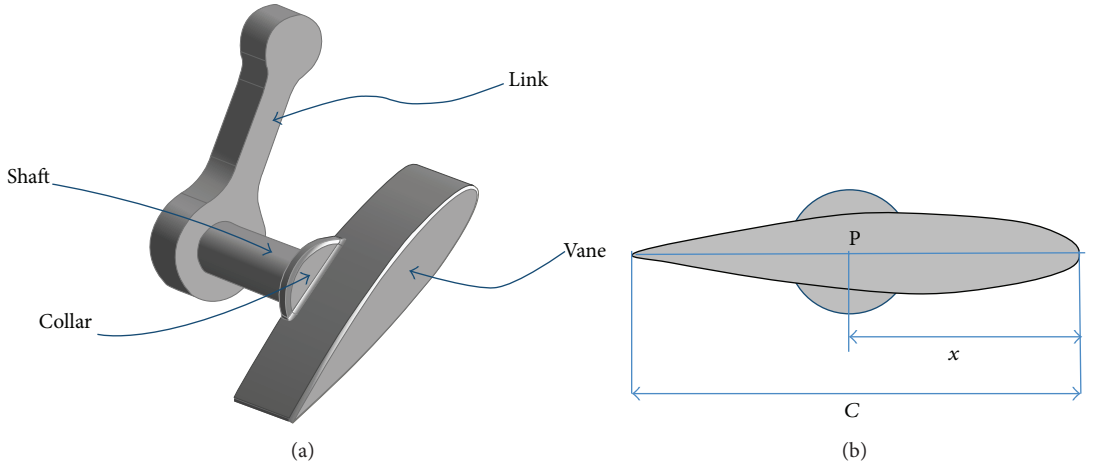

Figure 2: (a) Vane-shaft-link assembly and (b) location of pivot point P.

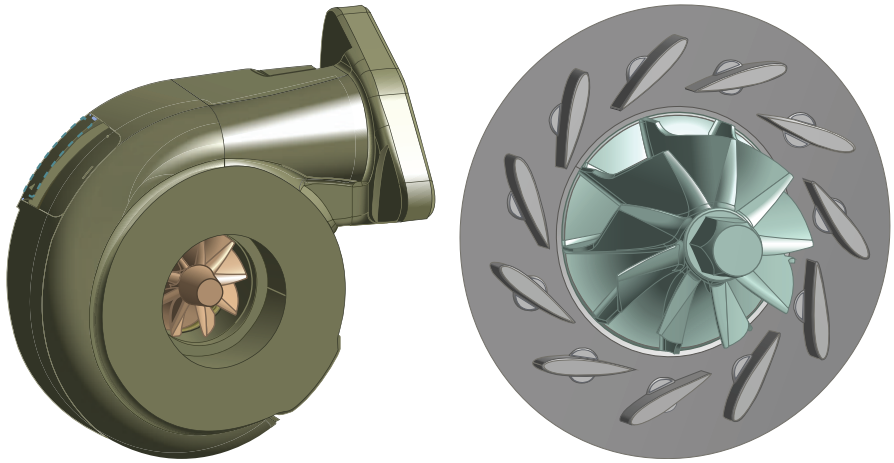

(a) Turbine housing and turbine wheel

(b) Turbine wheel with stator vane system

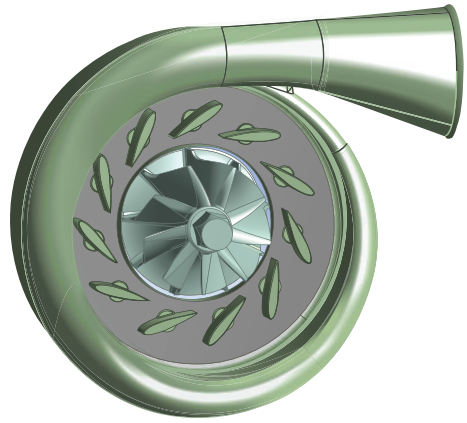

(c) Volute flow path extracted from housing

Figure 3: CAD model and computational domain.

CAD data for CFD analysis as shown in Figure 3. So, the computational model used for all the cases includes flow path in volute, around the stator vanes, around the rotor blades, and rotor downstream region. Additionally, to avoid numerical error, inlet and outlet boundaries are extended into straight pipes of length equal to five times the pipe diameter.

A three dimensional, steady state, turbulent analysis is performed using k-ω SST (shear stress transport) turbulence model developed by Menter [5]. Automatic wall function treatment was used to model the near wall physics. Automatic wall function approach switches from wall functions to a low Re near wall formulation according to the near wall mesh refinement. At the inlet, total pressure boundary condition with total temperature is applied. At the outlet, static pressure boundary condition is applied. The turbine wheel rotations are modeled using moving reference frame approach with frozen rotor interfaces.

All the cases were simulated and analyzed with 43 mm diameter radial inflow turbine wheel. The flow path through turbine wheel is modeled using hexahedral mesh with near wall refinement. All other regions are modeled using tetrahedral mesh with 12 prism layers near the wall as per the requirements of k-ω SST model to capture the boundary layer physics as accurately as possible. Grid independence test was performed to determine optimum free stream element sizes, first node distance from wall, and total mesh count to obtain grid independent solution.

Figure 4 shows the isentropic efficiency prediction with different mesh configurations shown in Table 1. The meshes having elements with minimum size lower than 0.12 mm, maximum size of 3 mm, first node distance from wall of 0.01 mm, and total mesh count greater than 6 million show same efficiency prediction. For different vane positions, the total element count including all the regions ranges from 6 to 8 million.

In order to understand the effect of vane shape on overall turbine performance across the complete turbine map, three pressure ratios with turbine speeds, namely, 1.4 with 93300 rpm (low), 1.8 with 124300 rpm (medium), and 2.4 with 151000 rpm (high) are chosen to represent the complete operating range. Simulations are performed at each of these pressure ratios with changing vane positions from min open to max open condition. Ten different vane positions are simulated between min and max open vane position to obtain results showing smooth variation of flow properties with vane position.

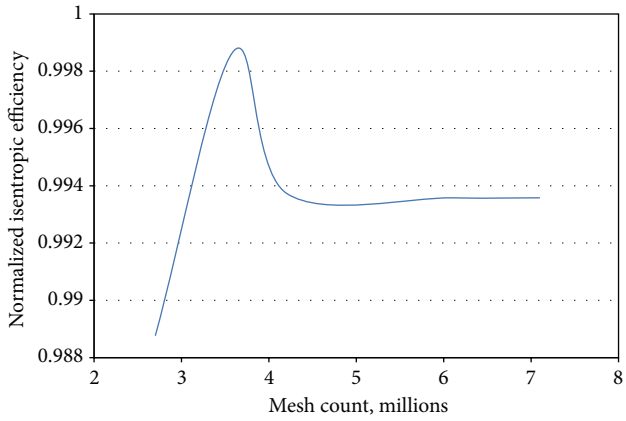

Figure 4: Grid independence test.

Table 1: Mesh configurations used for grid independent solution.

Min size mm	Max size mm	First node mm	Mesh count Millions
0.7	3.5	0.015	2.7
0.5	3.5	0.015	3.6
0.2	3	0.01	4.2
0.12	3	0.01	6.1
0.08	3	0.01	7.1

Turbine isentropic efficiency, aerodynamic vane opening torque, pressure drop across vanes, and turbine inlet relative flow angle variation with exhaust gas flow rate corresponding to vane position at each of the operating condition are compared for all the vanes.

5. Observations

At any particular inlet pressure and turbine speed, exhaust gas flow rate increases gradually as the vanes open. Based on exhaust gas flow rate, turbine performance can be approximately classified as "low end" and "high end" performance corresponding to the lower flow rate and higher flow rate conditions, respectively. Figure 5 shows typical velocity triangles at the turbine inlet. The triangle in Figure 5(a) is the case where whirl component of absolute velocity C_w is larger than the tip speed U of turbine wheel. This is seen during the low end operating conditions. Figure 5(b) is the case where tip speed is larger than whirl component of absolute velocity. This is seen during the high end operating conditions.

In VTG turbocharger, the absolute and relative flow angles at turbine inlet are expected to reduce with vane opening as shown by "expected path" in Figure 6. However, it has been observed that depending on the vane shape, the relative flow angle increases up to certain extent as the vane opens and then it reduces further as shown by the "actual path" in Figure 6. This behavior is attributed to the separated flow from one vane leading towards adjacent vane and influencing the flow over the adjacent vane when the vanes are in closed position, that is, at low end conditions. This interaction/mixing of flows from adjacent vanes affects overall flow direction and also causes loss in pressure energy, thus, affecting the turbine efficiency at these low end operating conditions. The point up to which the flow angle increases and after which it decreases can be termed as point of reversal.

According to different operating conditions, the vane opening and closing is controlled by the actuator. Actuator is appropriately chosen to apply sufficient force on the VTG system against the exhaust gas loads acting on the stator vanes for opening and closing. The exhaust gas load acting on vanes exerts aerodynamic torque on the vanes about pivot point P shown in Figure 7. This aerodynamic torque plays an important role in operating the actuator. The direction of aerodynamic torque determines the controllability of the actuator. It also determines whether the system is safe enough to continue its operation even in an event of actuator failure. A negative torque signifies the tendency of vane system to close due to gas loads and vice versa. It is expected that in the event of actuator failure, the vanes orient to fully open position, thus, avoiding any adverse effect on the engine operation.

It is not desired to have the aerodynamic torque changing its direction during the operation. Such change in direction of aerodynamic torque causes difficulty in controlling the operation of actuator. Further it is preferable to always have positive torque [4, 6] acting on the vanes which ensures the safety against actuator failure. While a positive torque is preferred, it is also desired that the magnitude of torque or gas loads acting on the vane are minimum to avoid excessive bending stress. The magnitude and direction of aerodynamic torque depends on shape of the vane which decides the flow incidence near vane LE.

The parameters such as vane PCD, x/C ratio, and the vane shape decide the extent to which it can be rotated for opening or closing between the min open and max open positions. With higher extent, smoother response of VTG system to different engine conditions can be expected. Further, the extent of opening also determines the maximum flow (capacity) that can be accommodated through the VTG system without choking. Higher extent of opening can be achieved easily by increasing the vane PCD. But, increase in vane PCD effects change in inflow condition to vane and also would require increase in overall size of the turbocharger. Thus, it is necessary to arrive at an optimum compromise between vane performance, controllability, and capacity of VTG system to deliver the best performance to the engine requirements.

6. Results and Discussions

For better clarity, all comparisons are made first among the symmetric vanes and then among symmetric vane 2 and asymmetric vanes.

The comparison of turbine isentropic efficiency variation with exhaust gas mass flow rate at low, medium, and high operating conditions for the five vanes mentioned before is shown in Figure 8. It can be seen that the reduction in

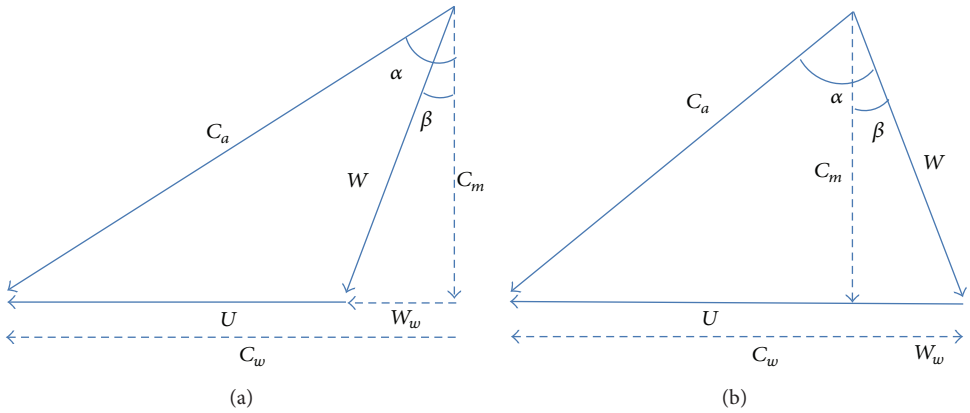

Figure 5: Turbine inlet velocity triangle.

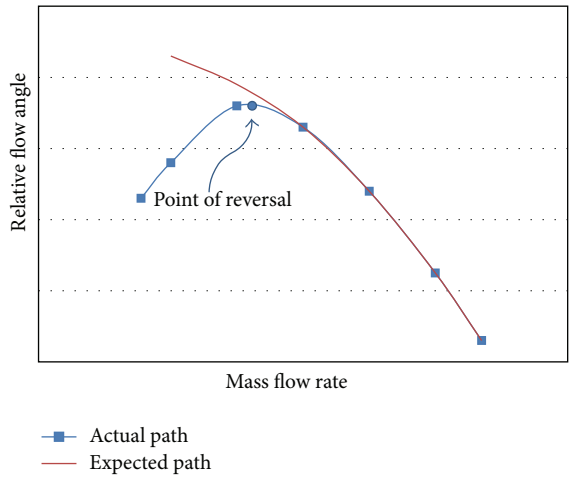

Figure 6: Expected and actual variation of relative flow angle with exhaust gas mass flow rate.

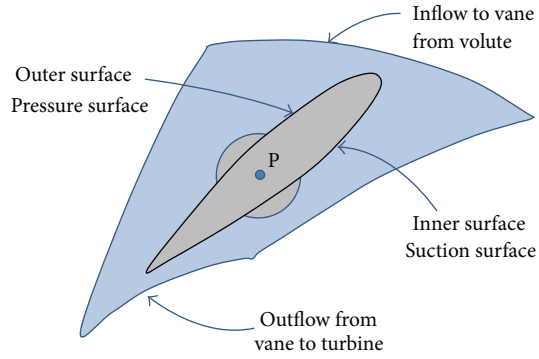

Figure 7: Single sector of the vane system.

thickness of straight vane (i.e., from symmetric vane 1 to symmetric vane 2) resulted in very marginal improvement in efficiency only at intermediate vane positions. The low and high end performance remained unchanged. Further, the increase in length along with reduction in thickness (i.e., from symmetric vane 1 to symmetric vane 3) also showed almost the same behavior. However, the use of asymmetric vanes has resulted in significant improvement of efficiency at low end as well as high end operating conditions. The improvement in efficiency with asymmetric vanes is higher at low end than at high end. Further, asymmetric vane 1 shows better efficiency than asymmetric vane 2 at low end, whereas asymmetric vane 2 shows better efficiency than asymmetric vane 1 at high end. This is because of the differences in pressure drop and relative flow angles between these two vanes.

The variation of turbine inlet relative flow angle with mass flow rate is shown in Figure 9. For all the vanes, as mentioned earlier, there exist points of reversal up to which the relative flow angle increases followed by gradual reduction. It can be seen that the point of reversal has shifted towards the upper-left side of the graph for asymmetric vanes signifying the reduction in vane opening angle up to which the vane-to-vane flow interaction/mixing existed. This reduction in vane-to-vane flow interaction/mixing reduces the pressure drop across the vane system at min open positions, thus, improving turbine efficiency. After point of reversal, the relative flow angle with asymmetric vanes appeared to be the same as symmetric vane.

Figure 10 shows velocity distribution around the vanes. It can be seen that the stagnation point for asymmetric vane 2 lies slightly off the leading edge towards pressure surface of the vane. However, symmetric vane 2 and asymmetric vane 1 show stagnation point nearer to the leading edge point. This causes asymmetric vane 2 to experience higher negative torque at the closed vane positions as shown in Figure 11 towards the lower mass flow rates. The upward nose provision of asymmetric vane 1 enables it to shift the stagnation point nearer to the leading edge point. Figure 12(b) shows the variation of pressure loads on vane surface from LE to TE on suction and pressure side. The pressure loads on pressure side are nearly same for all the three vane designs as all the vane designs are exposed to same upstream flow conditions emerging from volute. The drop in pressure load on pressure side towards TE due to vane-to-vane flow interaction near throat is also observed to be same in all vane designs as the x/C ratio and solidity ratio for all the vane designs is maintained nearly

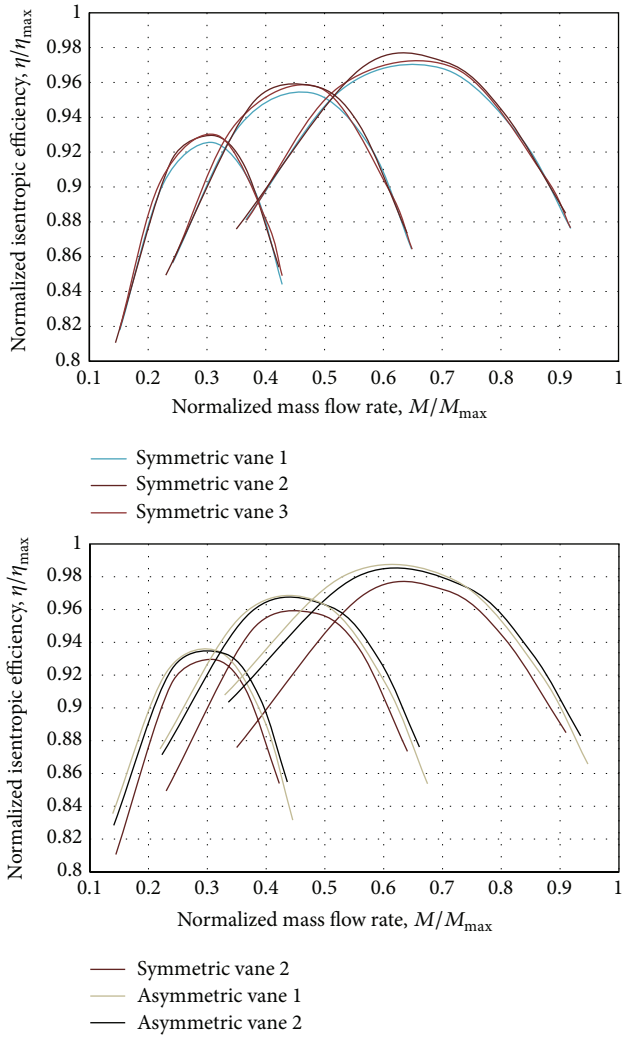

Figure 8: Variation of isentropic efficiency with mass flow rate.

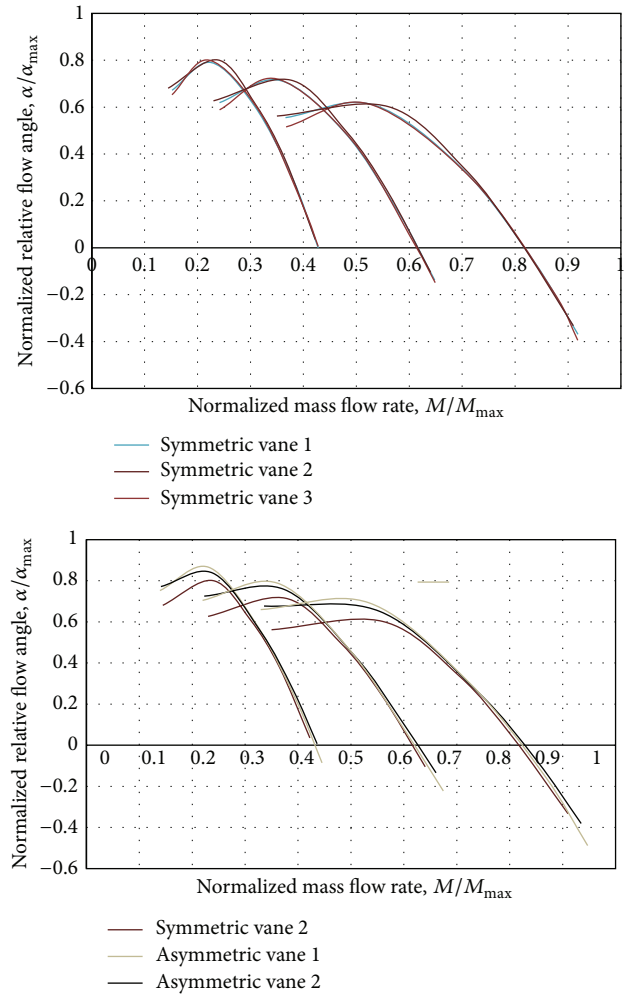

Figure 9: Variation of turbine inlet relative flow angle with mass flow rate.

same. Whereas, there exist differences in pressure loads on suction side which apart from stagnation point determines the superiority of one vane design over the other in its torque performance. Moreover, the pressure loads towards the LE and TE play major role than the loads near the pivot point in determining the direction of resultant torque. It can be observed that symmetric vane 2 experiences higher positive torque near LE and asymmetric vane 2 experiences the least. Asymmetric vane 1 experiences higher negative torque near TE and asymmetric vane 2 experiences the least. But, due to greater difference between positive and negative torque near TE, the differences in pressure loads there seem to be playing less important role in affecting the resultant torque direction. With the stagnation point location and with the observed pressure variations over the vane surfaces, the three vane designs experience different level of opening torques with symmetric vane 2 experiencing highest and asymmetric vane 2 experiencing the least.

The velocity distribution near the vane downstream region in Figure 10 and pressure distribution on the surface of the vane in Figure 12 show more gradual variation with asymmetric vanes as compared to symmetric vane. Further, it can be observed in Figure 12 pressure contour plots and pressure variation graph that on the suction surface of the vane near pivot point towards the TE, pressure loads on symmetric vane are lower than asymmetric vanes which confirms the higher loss of energy in case of symmetric vane due to flow interaction/mixing at that location. This vane-to-vane flow interaction not only causes pressure loss as shown in Figure 13 but also affects the relative flow angle delaying the point of reversal as shown in Figure 9.

Figure 13 shows the variation of pressure drop across vanes with exhaust gas mass flow rate. It can be seen that at low end as well as high end mass flow rates, the pressure drop across symmetric vane is higher than the asymmetric vanes at all operating conditions. The difference is more significant at low end. This reduction in pressure loss is effected by the reduction in vane-to-vane flow interactions/mixing coupled with aerodynamic drag reduction due to shape of the vane. Further it can also be noted that the pressure drop across asymmetric vane 1 is higher than asymmetric vane 2 at

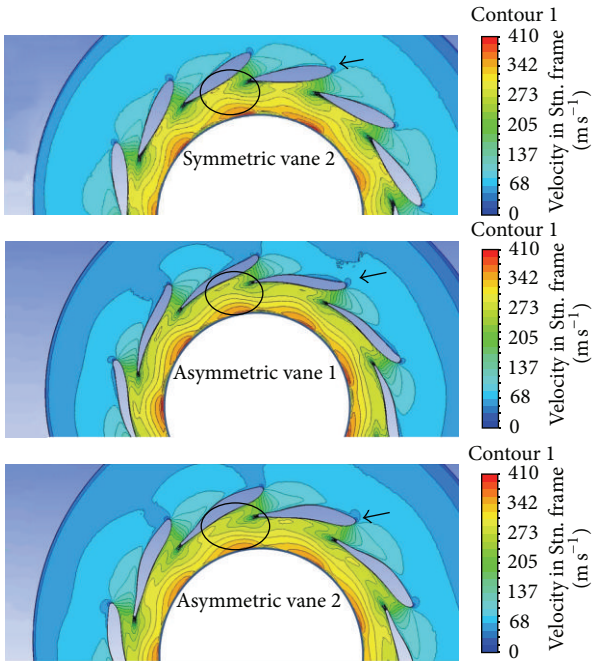

Figure 10: Velocity distribution around the vane.

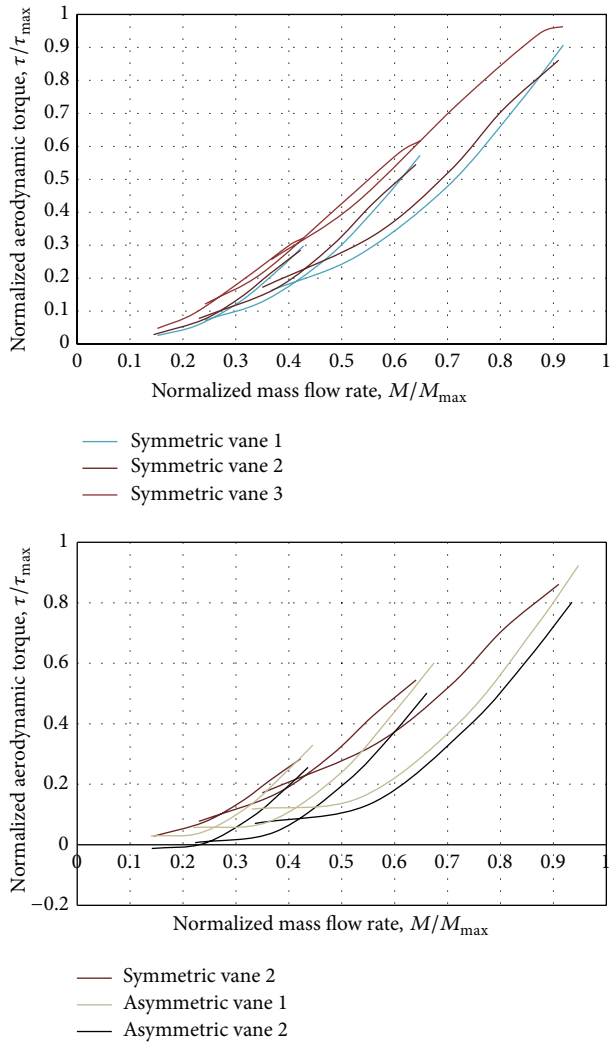

Figure 11: Variation of vane opening torque with mass flow rate.

high end mass flow rates which can be due to the upward nose provision of asymmetric vane 1 near leading edge causing local flow recirculation. At low end the upward nose provision is helpful in improving the angle of incidence, thus, reducing incidence losses.

Due to vane-to-vane flow interaction/mixing before point of reversal, the relative flow angle plays a less important role in determining the turbine efficiency than the pressure drop across vanes. Thus, gradual diversion of flow towards turbine wheel near trailing edge of the vane to minimize vane-to-vane flow interaction as achieved by asymmetric vanes improves turbine efficiency at min open positions. Further, it can also be understood that both relative flow angle as well as pressure drop influence the turbine efficiency after the point of reversal which can be seen with asymmetric vanes showing lower pressure drop across vanes and low relative flow angle as desired for achieving higher turbine efficiency.

Figure 11 shows the variation of resultant aerodynamic torque acting on vanes with mass flow rate. It can be observed that though use of symmetric vane yields lower turbine efficiency, it possesses better torque characteristics than asymmetric vanes. The aerodynamic torque with symmetric vane remains positive at all mass flow rates. However, the asymmetric vane 2 shows small amount of negative torque at low speed min open condition. With further vane opening, the direction of torque changes from negative to positive which can deteriorate controllability of actuator. On the other hand, it can be observed that the asymmetric vane 1 shows better torque characteristics in spite of nonsymmetric profile. This behavior of asymmetric vane 1 can be attributed to the upward nose provision existing near the leading edge. It is also observed that the upward nose provision in asymmetric vane 1 leads to local flow recirculation near max open positions which causes higher drag losses. Marginal loss in turbine efficiency near max open positions is witnessed due to the local flow recirculation in asymmetric vane 1 as shown in Figure 8.

According to Srithar and Ricardo [1], nozzle vanes experience higher pressure on suction surface than pressure surface, especially at closed positions due to upstream flow from the volute than the vane-to-vane flow interaction. It is observed that at closed vane positions, the pressure surface is directly exposed to the flow emerging from volute and thus it experiences higher pressure, whereas, suction surface shows variations in pressure distribution depending on the vane shape. It is also found that the shape of the vane influences the stagnation point location also apart from the pressure distribution. Asymmetric vane 1, for example, due to its upward nose provision receives the flow from volute with stagnation point nearer to LE point at min open positions achieving positive aerodynamic torque and better controllability of VTG system during operation.

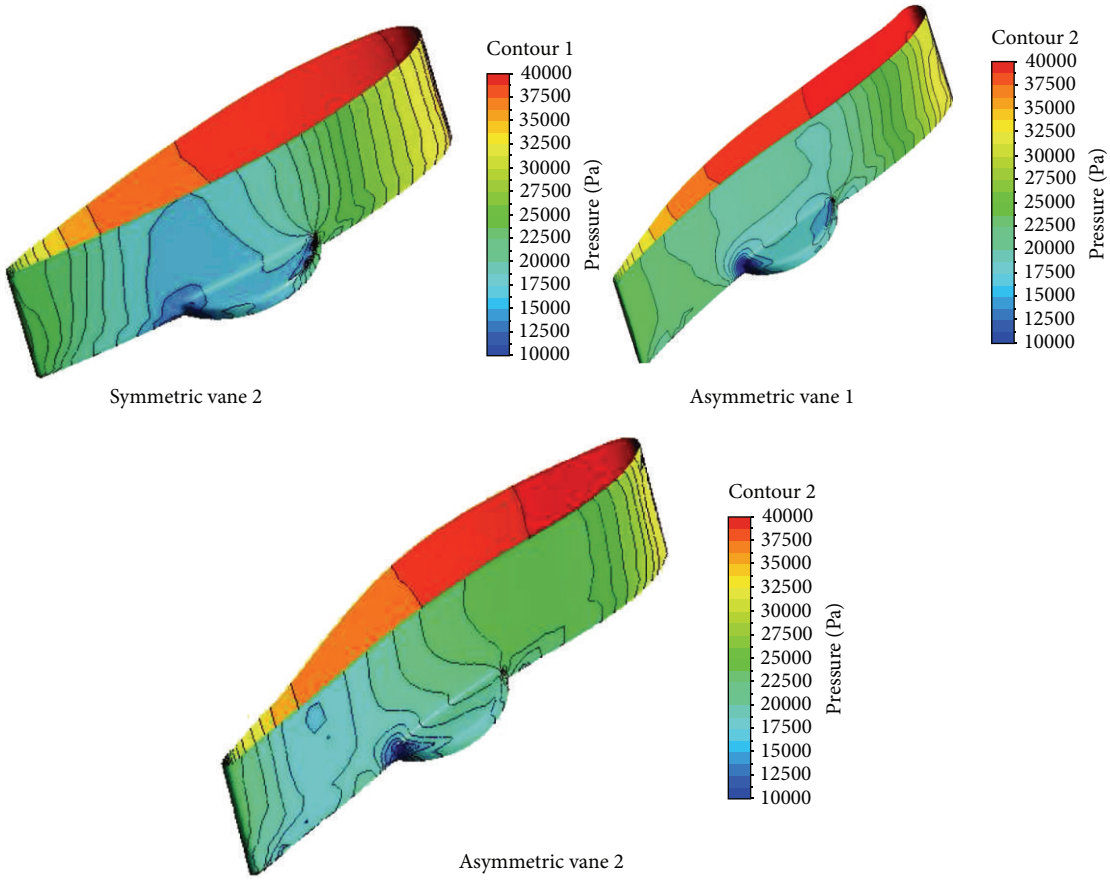

(a) Pressure variation contour plots

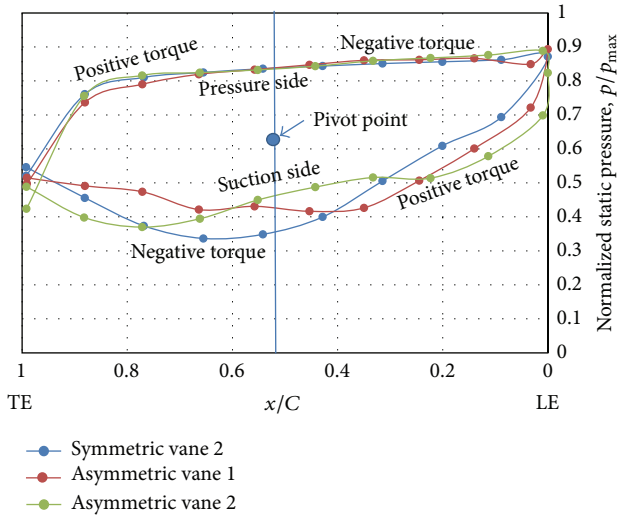

(b) Pressure variation graph

FIGURE 12: Pressure variation on vane surface.

7. Conclusion

Simulations are performed using three symmetric vane shapes and two asymmetric vane shapes. Asymmetric vanes show higher isentropic efficiency than symmetric vanes.

In VTG system operation, there exists a point of reversal up to which the relative flow angle increases with increasing vane opening. This point of reversal lies close to the min open position when the vanes are brought close to each other to reduce the gap between them. The increase in relative flow angle before point of reversal is due to vane-to-vane flow interaction/mixing. This interaction increases up to the point of reversal after which the flow from vanes is free to flow into the turbine wheel. The point of reversal for symmetric vanes

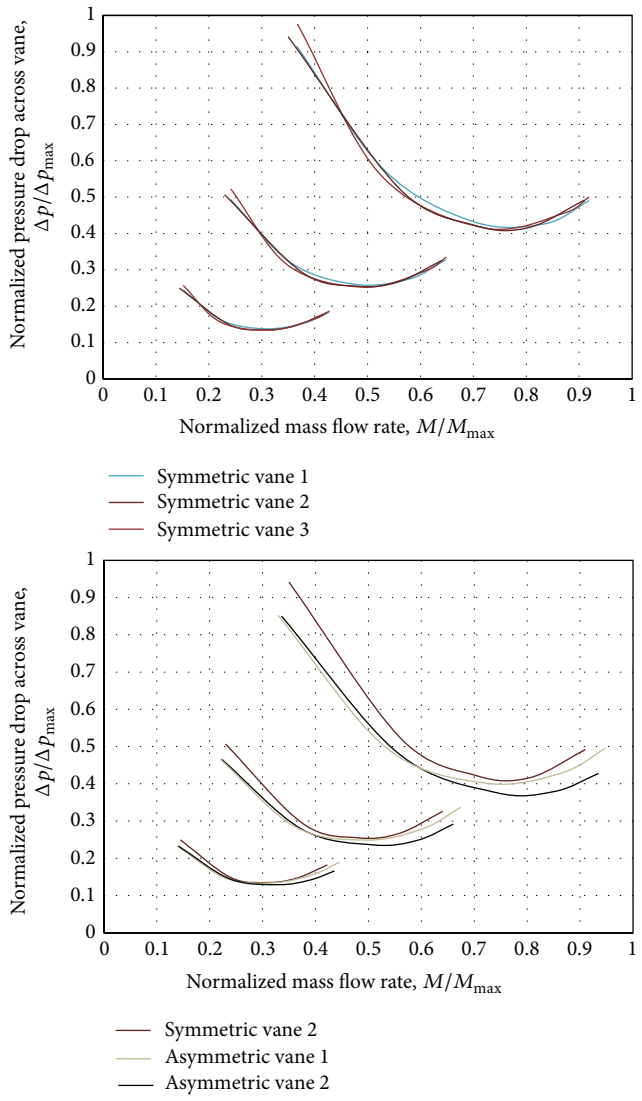

Figure 13: Variation of pressure drop across vanes with mass flow rate.

sustains for longer extent of vane opening than asymmetric vanes. Up to the point of reversal, the turbine efficiency depends only on the pressure drop caused across the vanes. After the point of reversal, it depends on relative flow angle at the turbine inlet as well as the pressure drop across vanes.

Though reduction in width of symmetric vane causes reduction in pressure drop across the vanes, the pressure drop at min open positions (before point of reversal) remains unchanged. The reduction in width does not improve relative flow angle. As a result, only marginal improvement in turbine efficiency is observed at intermediate vane positions.

The asymmetric vanes are found to be performing better than symmetric vanes due to the reduced pressure drop as well as improved relative flow angle. The use of asymmetric vanes reduces vane-to-vane flow interaction. This leads to reduction in pressure drop across vanes near minimum vane positions. The point of reversal is found to be sustaining for shorter extent of vane opening with asymmetric vanes, thus, significantly improving turbine efficiency at all the vane positions.

While the performance is improved by using asymmetric vanes, the gas forces acting on the vanes predominantly tend to apply negative aerodynamic torque which may cause the vanes to close in the absence of actuator. Moreover, the torque is found to be changing its direction near the minimum open positions. This reversal of aerodynamic torque can pose difficulty in smooth operation of VTG system. It is always desirable to have positive torque acting on the vanes at all vane positions [6]. The location of stagnation point along with the varying pressure loads over vane surface determines the direction resultant torque. It is observed that symmetric vane predominately experiences positive torque. Improved performance with controllability can be achieved by using asymmetric vanes by ensuring the point of stagnation to be near leading edge as far as possible accompanied by appropriate location of the vane shaft.

Nomenclature

α: Absolute flow angle, degrees
β: Relative flow angle, degrees
C: Chord, m
C_a: Absolute velocity, m/s
C_w: Absolute whirl velocity, m/s
C_m: Meridional velocity, m/s
T: Thickness, m
U: Tip speed, m/s
W: Relative velocity, m/s
W_w: Relative whirl velocity, m/s.

Abbreviations

BSFC: Brake specific fuel consumption
CFD: Computational fluid dynamics
EGR: Exhaust gas recirculation
LE: Leading edge
PCD: Pitch circle diameter, m
SST: Shear stress transport
TC: Turbocharger
VTG: Variable turbine geometry.

Conflict of Interests

The authors declare that there is no conflict of interests regarding the publication of this paper.

References

[1] R. Srithar and M.-B. Ricardo, "Variable geometry mixed flow turbine for turbochargers: an experimental study," *International Journal of Fluid Machinery and Systems*, vol. 1, no. 1, pp. 155–168, 2008.

[2] D. C. Eleni, T. I. Athanasios, and M. P. Dionissios, "Evaluation of the turbulence models for the simulation of the flow over a National Advisory Committee for Aeronautics (NACA) 0012 airfoil," *Journal of Mechanical Engineering Research*, vol. 4, no. 3, pp. 100–111, 2012.

[3] A. T. Simpson, S. W. T. Spence, and J. K. Watterson, "A comparison of the flow structures and losses within vaned and vaneless stators for radial turbines," *ASME Journal of Turbomachinery*, vol. 131, no. 3, Article ID 031010, 2009.

[4] L. Hu, C. Yang, H. Sun, J. Zhang, and M. Lai, "Numerical analysis of nozzle clearance's effect on turbine performance," *Chinese Journal of Mechanical Engineering*, vol. 24, no. 4, pp. 618–625, 2011.

[5] F. R. Menter, "Two-equation eddy-viscosity turbulence models for engineering applications," *AIAA journal*, vol. 32, no. 8, pp. 1598–1605, 1994.

[6] P. Renaud and D. Tisserant, "Variable Nozzle Turbocharger," United States Patent Pub. No. US 2008/0131267 A1, pp 1, line [0008], 2008.